Time-frequency methods in time-series data analysis

Paulo Gonçalvès[1], Patrick Flandrin[2], Eric Chassande-Mottin[2]

[1] INRIA Rocquencourt
Projet FRACTALES
Domaine de Voluceau, BP 105, 78153 Le Chesnay Cedex, France.
E-mail: Paulo.Goncalves@inria.fr
[2] Ecole Normale Supérieure de Lyon
*Laboratoire de Physique (*URA 1325 CNRS*)*
46 allée d'Italie, 69364 Lyon Cedex 07, France
E-mail: {echassan, flandrin}@physique.ens-lyon.fr

Abstract. The aim of this paper is to review some basics on time frequency analysis. Starting with linear decompositions, a natural generalization of the Fourier transform, we then present different classes of bilinear energetic distributions and their reassigned extensions. We finally motivate the interest of these tools, showing how they can help at simplifying some signal processing schemes, with special emphasis on the detection problem. All along the paper, the Newtonian model for a certain type of gravitational waves serves as an illustrative example.

1 Time versus frequency representations

1.1 The Shannon and Fourier representations of a signal

The Shannon representation. One very natural way of describing a signal x[1] is to use its time representation,

$$x(t) \;=\; \int x(u)\,\delta(u-t)\,du \;=\; \langle x, \delta_t \rangle, \tag{1}$$

where $\delta(t)$ is the Dirac distribution localized at time $t = 0$. This representation is also referred to as the Shannon expansion and corresponds to the expansion of the observation x onto a continuous basis generated by a set of time-shifted versions of a perfectly time-localized analyzing function.
Then, the Shannon representation appears very natural as it depicts the signal in terms of waveforms which carry most of the information about the physical system that originated the observation. The example presented in figure 1–a shows the expected gravitational waveform produced by the coalescence of a

[1] In this paper, we deal with the vector space $L^2(T)$ of finite energy signals $\int_0^T |x(u)|^2\,du < +\infty$, where T is the observation interval. Also, we consider time signals, which means that the observation space (or direct space) is parameterized by the time variable.
Unless specified, integrals run from $-\infty$ to $+\infty$.

massive binary system, under Newtonian approximations. This wave corresponds to the real part of the complex-valued signal [11] :

$$x(t;t_0,d) \;=\; A\,(t_0-t)^{-\alpha}\,e^{-i2\pi d(t_0-t)^{\beta}}\,U(t_0-t), \tag{2}$$

with U the Heavyside step function, $\alpha = 1/4$, $\beta = 5/8$, t_0 the coalescence time and d, A physical constants. This example clearly evidences that the instantaneous amplitude of the signal envelope increases with time while the period of the oscillations converges toward zero as we reach the coalescence time.

The Fourier representation. Another very standard and useful way of representing a signal x is the so-called Fourier representation obtained via the Fourier transform :

$$X(f) = \int x(u)\,e^{-i2\pi fu}\,du \;=\; \langle x, e_f\rangle. \tag{3}$$

This transform decomposes the signal x onto a set of pure harmonics $\{e_f\}_{f\in\mathbb{R}}$ which, in contrast with the Dirac functions of the Shannon representation, are functions with infinite support in time and perfectly localized in the frequency domain (i.e. $\langle e_{f_0}, e_f\rangle \;=\; \delta(f-f_0)$). Then, $X(f)$, a complex-valued function in general, yields an harmonic description aimed at identifying the spectral content of the signal x : the squared magnitude $|X(f)|^2$, referred to as the spectrum of x, quantifies the energetic contribution of each harmonic e_f, whereas $\mathrm{Arg}(X(f))$, the phase spectrum, gives the relative phase of each one of these components. Moreover, the inverse Fourier transform, given by :

$$x(t) = \int X(f)\,e^{+i2\pi ft}\,df, \tag{4}$$

defines a one-to-one correspondence between the time representation of a signal and its frequency representation (equality in (4) is w.r.t the L^2 norm). As a corollary of this unitary mapping, the Parseval formula :

$$\langle x, y\rangle \;=\; \int x(t)y^*(t)\,dt \;=\; \int X(f)Y^*(f)\,df, \tag{5}$$

preserves the inner product in the signal space $L^2(\mathbb{R})$.

In the case of the gravitational waves (2), using a stationary phase argument, it is possible to approximate the Fourier integral in (3) to get [2] :

$$X_{r,k}(f) = C\,f^{-(r+1)}\,e^{i\Psi_k(f)}\,U(f), \tag{6}$$

where $\Psi_k(f) = -2\pi\left(cf^k + t_0 f + \gamma\right)$, $k = -5/3$ and $r = 1/6$. Figure 1–b represents the corresponding energy spectrum $|X_{r,k}(f)|^2$ in a bilogarithmic plot. Although it features the frequency extent of the signal and the power law decay of the energy spectrum, this plot masks the non-stationarity initially evidenced by the time waveform of figure 1–a (indeed, this information is contained only in the phase spectrum of (6)).

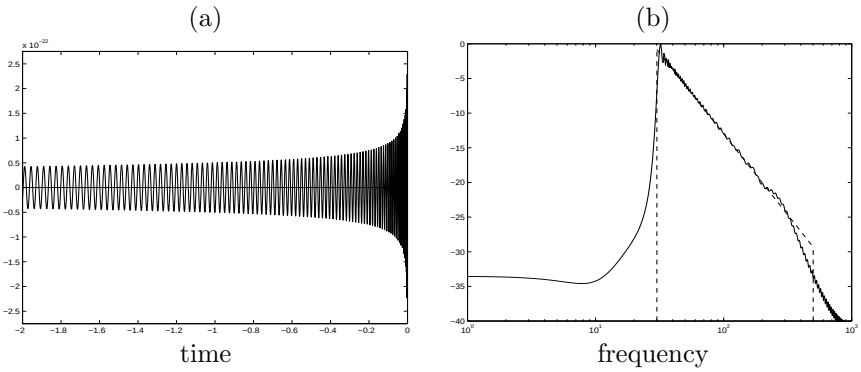

Figure 1: (a) Time representation of the gravitational waveform (2). (b) Frequency spectrum: square magnitude of (6) in a *Log-Log* plot.

1.2 Instantaneous frequency and group delay

Instantaneous frequency. In order to capture non-stationarities of the frequency content of a real signal x, the *instantaneous frequency* is defined on its associated analytic signal[2] $x_a(t) \;=\; a(t)\, e^{i\varphi(t)}$ as follows:

$$f_x(t) \;=\; \frac{1}{2\pi}\frac{d\varphi(t)}{dt}. \tag{7}$$

In particular, for mono-component signals (i.e. signals existing only around one frequency at each time), this definition allows to characterize the frequency behavior of x locally in time; as a result, the graph of f_x *vs.* time t can be interpreted as a joint time-frequency signature of x.

Group delay. Conversely, a dual expression of the instantaneous frequency, aimed at describing the time behaviour locally in frequency exists: it corresponds to the *group delay*. It relies on the phase spectrum of the Fourier transform $X(f) \;=\; B(f)\, e^{i\Psi(f)}$ as follows:

$$t_x(f) \;=\; -\frac{1}{2\pi}\frac{d\Psi(f)}{df}. \tag{8}$$

In general, instantaneous frequency and group delay are not reciprocal functions. Yet, for large time bandwidth product signals, the approximation $t_x(f_x(t)) \sim t$ holds, validating to consider indifferently one of the two functions [5].

Following our example of gravitational waves (6), the group delay reads $t_x(f) \;=\; t_0 + ckf^{k-1}$, and justifies why (6) is named *power law chirp signal*. Now, assuming large time bandwidth product [2], an expression for the instantaneous frequency is inferred from $t_x(f)$ and plotted in figure 3–a. It

[2]The Fourier transform $X(f)$ of a real signal is related to the Fourier transform $X_a(f)$ of its associated analytic signal by $X_a(f) \;=\; 2X(f)U(f)$.

defines a power law trajectory in the time-frequency plane that features the non-stationary behaviour of the frequency content of x.

At this point, let us emphasize that one major proviso in exploiting instantaneous frequency (or group delay) is the requirement of mono-component signals. In practice, not only this condition is rarely satisfied but also observations are usually corrupted with additive noise, making definitions (7) and (8) numerically instable.

2 Atomic joint time-frequency representations

Atomic decompositions rely on a linear decomposition of the signal onto a set of elementary analyzing functions as [5]:

$$\Gamma_x(t,f;g) \;=\; \langle x, g_{t,f}\rangle, \quad \forall t \in T,\, \forall f \in \mathbb{R}. \tag{9}$$

The key-point in (9) is that the entire analyzing set $\{g_{t,f}\}$ is generated by a unique prototype function g_0, which in contrast with the Dirac and harmonic functions of the Shannon and Fourier representations, are well-localized in time and frequency simultaneously. To get $\{g_{t,f}\}$, g_0 is duplicated around each position $(t,f) \in (T \times \mathbb{R})$, by means of a time and frequency displacement operators pair[3], rather than just a shift in time or frequency as it was the case in (1) and (3) respectively.

Atomic framework allows for a host of different decompositions with specific characteristics, depending on both the choice of the time-frequency displacement operator, and g_0. A particularly interesting property stems from selecting a normalized analyzing function $\int |g_0(t)|^2\, dt = 1$, which in turn produces a decomposition $\Gamma_x(t,f)$ that preserves the energy E_x of the signal according to:

$$\iint |\Gamma_x(t,f;g)|^2\, dt\, df \;=\; \int |x(t)|^2\, dt \;=\; \int |X(f)|^2\, df \;=\; E_x. \tag{10}$$

$|\Gamma_x(t,f;g)|^2$ corresponds to an *energetic time-frequency representation* (TFR), or time-frequency distribution of x [6, 5].

Atomic decompositions support a very simple implementation, yet they suffer a severe limitation: since analyzing function g_0 has finite equivalent supports Δt_{g_0} in time and Δf_{g_0} in frequency, it precludes to obtain a linear decomposition with arbitrarily high resolutions, in accordance with the uncertainty principle $\Delta t_{g_0} \Delta f_{g_0} \geq 1/4\pi$.
We now review two popular examples.

Short time Fourier transform. The short time Fourier transform (STFT) combines time shift and frequency shift operators used separately in representations (1) and (3), in a sole decomposition:

$$\Gamma_x(t,f;g) \;=\; \int x(u)\, g_0^*(u-t)\, e^{-i2\pi f u}\, du, \quad (t,f) \in (T \times \mathbb{R}), \tag{11}$$

[3]It is possible to restrict the action of the operators only to a discrete sampling of the plane $(T \times \mathbb{R})$, yielding to discrete linear decompositions.

where g_0 is a low-pass prototype function. This particular displacement operator corresponds to the uniform time-frequency tiling schematized in figure 2–c.

Basically, we can interpret the STFT (11) as a Fourier transform (3) applied to the windowed signal $x(u)\, g_0(u-t)$. By limiting the time support of x around each time t, the STFT permits to track non-stationarities on the signal, such as frequency shifts or transients.
Returning to our example of gravitational waves, we compute (11) using a Gaussian window g_0. The spectrogram (the energy distribution resulting from squaring the magnitude of the STFT coefficients) concentrates around the instantaneous frequency of the signal (see figure 3–b).
Continuous wavelet transform. Coupling time-shift operator with scale change operator yields another interesting atomic decomposition. Introduced as the continuous wavelet transform (CWT) [9]:

$$\Gamma_x(t,f;g) \;=\; \int x(u) \left(\frac{f}{f_0}\right)^{\frac{1}{2}} g_0^* \left(\frac{f}{f_0}(u-t)\right) du, \quad (t,f) \in (T \times \mathbb{R}_+^*), \quad (12)$$

this linear decomposition relies on the so-called analyzing mother wavelet g_0, an oscillating function with frequency f_0. Formally, for g_0 to give rise to a valid TFR (i.e. one can recover the signal x by inverting $\Gamma_x(t,f;g)$), it must satisfy to the following admissibility condition:

$$\int \frac{|G_0(\nu)|^2}{|\nu|}\, d\nu \;=\; 1, \quad (13)$$

where $G_0(\nu)$ stands for the Fourier transform of g_0. Then, whenever (13) holds, the CWT partitions the time-frequency plane according to the constant relative bandwidth tiling showed in figure 2–d. In contrast with the STFT, the CWT offers a joint time and frequency resolution that varies naturally with the analyzed frequency, matching to physical situations for which a scale based analysis is more relevant than a spectral representation.
Using a modulated Gaussian wavelet (Morlet wavelet), we compute (12) on the gravitational wave (2), the resulting energy representation (scalogram) is presented at (figure 3–c).

3 Energetic bilinear distributions

3.1 Definition

Lack of good time-frequency localization properties of atomic decompositions have prompted the development of more advanced bilinear distributions. These distributions can be viewed as a generalization of the squared magnitude of a linear decomposition:

$$|\Gamma_x(t,f;g)|^2 \;=\; \iint x(u)\, x^*(v)\, g_{t,f}(u)\, g_{t,f}^*(v)\, du\, dv, \quad (14)$$

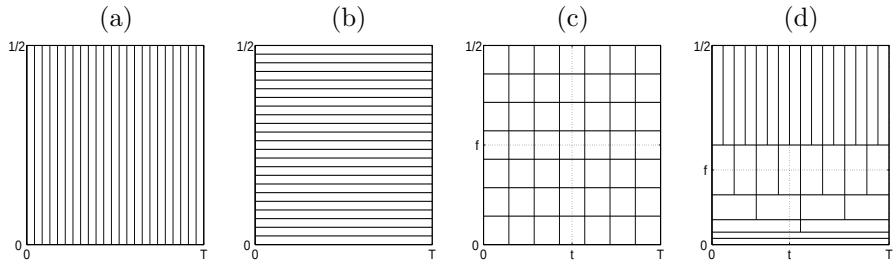

Figure 2: Time frequency patterns corresponding to different signal representations. X–axis corresponds to time, Y–axis corresponds to frequency. (a) Shannon representation. (b) Fourier representation.(c) Short time Fourier transform .(d) Wavelet transform.

where the specific term $(g_{t,f}(u)\, g^*_{t,f}(v))$ is replaced by a more general arbitrary kernel $K(u,v;t,f)$, to get [6, 5]:

$$\rho_x(t,f;K) \;=\; \iint x(u)\, x^*(v)\, K(u,v;t,f)\, du\, dv. \tag{15}$$

This canonical definition offers a large flexibility in the choice of K and more interestingly, it is possible to translate each theoretical property of ρ_x in terms of an admissibility constraint on K. For instance, for $\rho_x(t,f;K)$ to be an energy distribution satisfying to:

$$\iint \rho_x(t,f;K)\, dt\, df \;=\; \int |x(t)|^2\, dt \;=\; \int |X(f)|^2\, df \;=\; E_x, \tag{16}$$

K needs to obey the following marginal condition:

$$\iint K(u,v;t,f)\, dt\, df \;=\; \delta(u-v). \tag{17}$$

Thereafter, we only consider distributions of this type. Another particularly interesting property to impose on ρ_x, is the covariance with respect to some time-frequency displacement operator T; more precisely, we want the following diagram to be commutative:

$$\begin{array}{ccc} x(t) & \longrightarrow & Tx(t) \\ \downarrow & & \downarrow \\ \rho_x(t,f\,;K) & \longrightarrow & \rho_{Tx}(t,f\,;K) = T\rho_x(t,f\,;K). \end{array} \tag{18}$$

In fact, this constraint is used as a starting point to reduce the wide class of bilinear TFRs (15) to less general, yet extensive, sub-classes. So, following this approach, we consider successively the two displacement operators defined in (11) and (12), to generate two important classes of TFRs: the Cohen class and the affine class.

3.2 The Cohen class of time-frequency distributions

The Cohen class is defined as the set of all bilinear time frequency distributions that are covariant with respect to time-shift and frequency-shift operations [6] :

$$\begin{array}{ccc} x(t) & \longrightarrow & x(t-t_0)\, e^{i2\pi f_0 t} \\ \downarrow & & \downarrow \\ \rho_x(t,f;K) & \longrightarrow & \rho_x(t-t_0, f-f_0; K). \end{array} \tag{19}$$

Thus, any distribution (15) satisfying to this principle simplifies to a two dimensional convolutive form :

$$C_x(t,f;\Pi) \;=\; \iint W_x(u,\theta)\, \Pi(u-t,\theta-f)\, du\, df, \tag{20}$$

of the so-called Wigner distribution :

$$W_x(t,f) \;=\; \int x\left(t+\frac{\tau}{2}\right)\, x^*\left(t-\frac{\tau}{2}\right)\, e^{-i2\pi f\tau}\, d\tau, \tag{21}$$

with an arbitrary 2D parameterizing kernel Π. The Wigner distribution plays a key-role for this class, and satisfies to several theoretical properties that can carry on to other members of the class conditionally to proper choices of K [6, 5]. Among these properties, is the strict localization on linear chirp signals of the form $x(t) = \exp\{i2\pi(\beta t^2/2 + f_0 t)\}$. For these FM signals we have $W_x(t,f) = \delta(f-(f_0+\beta t))$, concentrating perfectly on the linear instantaneous frequency trajectory.

The Wigner distribution is unitary, which means that it preserves the inner product from $L^2(\mathbb{R})$ to $L^2(\mathbb{R}^2)$ according to the Moyal formula :

$$\left|\int x(t)\, y^*(t)\, dt\right|^2 \;=\; \iint W_x(t,f)\, W_y(t,f)\, dt\, df. \tag{22}$$

Whereas the mapping $x \mapsto C_x$ is not an isometry in general, Eq. (22) holds for C_x if and only if the associated kernel Π verifies the condition : $|\Phi(\tau,\xi)| = 1$, where Φ is the Fourier transform of Π. This fundamental property, along with the covariance principle (19) provides us with a time-frequency counterpart of any convolution-based signal processing. In this direction, it becomes trivial to demonstrate that the spectrogram, defined as the squared magnitude of a STFT, is a particular member of the Cohen class and corresponds to the 2D low-pass kernel $\Pi(t,f) = W_{g_0}(t,f)$ in (20).

Figure 3–d illustrates the Wigner distribution computed on the gravitational wave signal of (2). Although it overtakes the spectrogram in terms of localization on the power law group delay itself, the Wigner distribution develops noxious oscillating components, referred to as interference terms, inherited from the bilinearity of its definition (21) [5]. For its part, the spectrogram, as a smoothed version of the Wigner distribution, removes all zero-mean interference terms while spreading out the auto-components.

3.3 The affine class of time-frequency distributions

Selecting time shifts and scale changes rather than time and frequency shifts, yields *mutatis mutandis* the affine class of TFRs that satisfy to the new covariance diagram :

$$\begin{array}{ccc} x(t) & \longrightarrow & |a|^{-1/2}\, x\left(\frac{t-t_0}{a}\right) \\ \downarrow & & \downarrow \\ \rho_x(t,f;K) & \longrightarrow & \rho_x\left(\frac{t-t_0}{a}, af\,;\,K\right). \end{array} \tag{23}$$

In [4], it is proved that for all affine Wigner distributions $P^{(k)}$ of this class, there exist a real k and a continuous non-vanishing parameterizing function μ_k such that[4] :

$$P_X^{(k)}(t,f) \;=\; f^{2(r+1)-q} \int \mu_k(u)\, X(f\lambda_k(u))\, X^*(f\lambda_k(-u))\, e^{i2\pi t f \zeta_k(u)}\, du, \tag{24}$$

with $\lambda_k(u) = \left(k(e^{-u}-1)/(e^{-ku}-1)\right)^{1/(k-1)}$, $\forall k \neq 0,1$; $\lambda_0(u) = u/(1-e^{-u})$; $\lambda_1(u) = \exp\left(1+(u\,e^{-u})/(e^{-u}-1)\right)$; $\zeta_k(u) = \lambda_k(u) - \lambda_k(-u)$, and r, q two real-valued constants. As we saw, Wigner distribution is naturally adapted to linear chirp signals ; similar localization properties generalize to affine Wigner distributions when applied to power law chirp signals of the form $\{X_{r,k}(t) = C\, f^{-(r+1)}\, e^{i\Psi_k(f)}\, U(f) \;:\; t_{x_k}(f) = t_0 + ck\, f^{k-1},\, k \in \mathbb{R}^*_-\}$. In that case, the distribution $P^{(k)}$, with same k as in $X_{r,k}$, behaves as :

$$P^{(k)}_{X_{r,k}}(t,f) = C^2 f^{-(q+1)}\, \delta(t - t_{x_k}(f)) \;\;\Leftrightarrow\;\; \mu_k^L(u) = \frac{d\zeta_k(u)}{du}(\lambda_k(u)\,\lambda_k(-u))^{r+1}. \tag{25}$$

One can either establish this result by a straightforward calculus as in [4], or use geometric arguments to show that power law trajectories are the eigenstructures (i.e. globally invariant) of the pointwise construction rules that underlie affine Wigner distributions [8].

Looking back to our example, we know that, in first approximation, a gravitational wave model produced by the coalescence of a massive binary system exhibits a $k = -5/3$ power law group delay. Accordingly, the affine Wigner distribution $P^{(-5/3)}$, along with the specific choice (25) for μ_k perfectly localizes on the time frequency path $t_x(f) = t_0 + cf^{-5/3}$ (see figure 3–e).[5]

As far as unitarity is concerned, a Moyal formula similar to (22) holds for any affine Wigner distribution (24) associated to the following parameterizing function [4] :

$$\mu_k^U(u) \;=\; \left(\frac{d\zeta_k(u)}{du}\right)^{\frac{1}{2}} \left(\lambda_k(u)\,\lambda_k(-u)\right)^{r+1}. \tag{26}$$

Surprisingly, only for $k = 0$ we have $\mu_0^U(u) = \mu_0^L$, leading to the unique distribution $P^{(0)}$ that satisfies to localization on hyperbolic paths and to unitarity

[4] An equivalent canonical definition of this class is proposed in [7], relying on an affine convolution of the Wigner definition.

[5] We used a pseudo affine Wigner distribution algorithm proposed in [10] to estimate $P_X^{(k)}$.

simultaneously. Nevertheless, although a localized (active) distribution $P^{(k)}$ is not unitary in general, it cooperates with its passive form [4, 2]:

$$\widetilde{P}_X^{(k)}(t,f) = \int \Psi_k(f(t-\tau))\, P_X^{(k)}(\tau,f)\, d\tau \quad \text{with} \quad \Psi_k(s) = \int e^{i2\pi s\zeta_k(u)}\, du, \quad (27)$$

to produce an isometry-like relation of the form:

$$\left| \int_0^{+\infty} X(f)\, Y^*(f)\, f^{2r+1}\, df \right|^2 \;=\; \iint_0^{+\infty} \widetilde{P}_X^{(k)}(t,f)\, P_Y^{(k)}(t,f)\, f^{2q}\, df\, dt. \quad (28)$$

Starting from this relation, and applying the affine covariance of diagram (23) to the CWT (12), it is straightforward to rewrite the scalogram (squared magnitude of the CWT) as:

$$|\Gamma_x(t,f;g)|^2 = \iint_0^{+\infty} \widetilde{P}_X^{(k)}(u,\theta)\, P_{G_0}^{(k)}\left(\frac{f}{f_0}(u-t), \theta\frac{f_0}{f}\right) \theta^{2q}\, d\theta\, du. \quad (29)$$

The scalogram is a particular member of the affine class of TFR and it can be interpreted as a frequency-dependent smoothed version of an affine Wigner distribution with kernel $P_{G_0}^{(k)}$. Conversely, quadratic *affine Wigner distributions* are high resolution alternatives to the wavelet transform. They have many desirable theoretical properties but, unfortunately, also two primary drawbacks. First, their bilinearity results in copious interference terms in the time-frequency plane (except for the eigen-structures $X_{k,r}$). Second, as the entire signal enters their definition, efficient implementations suitable for long time series have not been developed for most of these TFRs [10]. As a result, few affine Wigner distributions have been employed in real-world applications.

4 Reassignment methods

Concurrently to the previous approach, Kodera *et al.* [12] proposed another method to obtain well-localized TFRs. Their approach, referred to as *reassignment*, is based on a post-processing of the spectrogram. It consists in moving the values of the spectrogram from their initial computation point to a time-frequency location $(\hat{t}(t,f),\, \hat{f}(t,f))$ given by a local center of mass computed over the Wigner-Ville distribution of the signal. This results in a squeezing of each signal components along their associated group delay and/or instantaneous frequency path. This is illustrated in figure 3–f with the reassigned spectrogram of a gravitational wave. Moreover, reassignment has been proved [1] to rely on a more general concept and therefore can be extended to all distributions of Cohen and affine classes.

From a computational viewpoint, the reassigned spectrogram supports efficient algorithms based on a companion expression for the reassignment point coordinates [1]:

$$\begin{array}{rcl} \hat{t}(t,f) & = & t + \mathrm{Re}\left\{\Gamma_x(t,f\,;\, t.g)/\Gamma_x(t,f\,;\,g)\right\} \\ \hat{f}(t,f) & = & f - \mathrm{Im}\left\{\Gamma_x(t,f\,;\, dg/dt)/\Gamma_x(t,f\,;\,g)\right\}. \end{array} \quad (30)$$

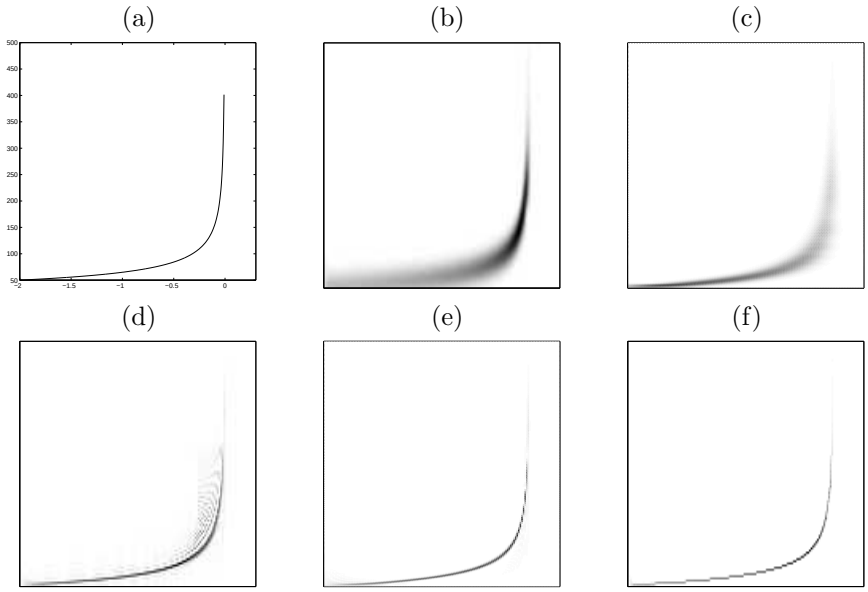

Figure 3: Time-frequency energy distributions computed on the gravitational wave defined in (2). X-axis corresponds to time and Y-axis to frequency. (a) Theoretical law as given by the instantaneous frequency (7). (b) Spectrogram, the squared magnitude of the STFT (11). (c) Scalogram, the squared magnitude of the CWT (12). (d) Wigner-Ville distribution (21). (e) Affine Wigner distribution (24) with $k = -5/3$. (f) Reassigned spectrogram (see Sect. 4)

Therefore, the resulting algorithm combines in a proper way, three STFTs of the signal based on three distinct windows.

5 Beyond analysis

TFRs, not only perform remarkably well when applied to non-stationary signals, but also allow to advantageously reformulate some standard signal processing operations such as detection, estimation or identification. Although no performance gain is to be expected from this approach, peculiar properties of TFRs can serve as to simplify their implementation in a dramatic way. It is for instance the case for detection, where the problem at hand is to identify a signal x_θ, completely determined save for some unknown parameter θ (e.g. arrival time), in a noise-corrupted observation y. It is then well-known that the squared output of the matched filter (expressed in the frequency domain) :

$$\Lambda(y;\theta) \;=\; \left|\langle Y, X_\theta\rangle\right|^2, \tag{31}$$

defines the generalized likelihood ratio test (GLRT) [2], which is maximum over θ, when the prototype signal X_θ coincides with the observation Y. Using the

Moyal-type formula (28) for localized affine Wigner distributions, Eq. (31) is then equivalent to :

$$\Lambda(y;\theta) \;=\; \langle\langle \widetilde{P}_Y^{(k)}, P_{X_\theta}^{(k)} \rangle\rangle. \tag{32}$$

If, in addition, X_θ corresponds to the eigen-structure $X_{k,r}$ on which $P^{(k)}$ perfectly concentrates, the GLRT of Eq. (31) simply reduces to the time-frequency path integration :

$$\Lambda(y;\theta) = \int\!\!\int_{\mathbf{R}_+} \widetilde{P}_Y^{(k)}(t,f)\, \delta(t - t_{x_\theta}(f)) f^{2q}\, df\, dt. \tag{33}$$

This example emphasizes the role of localized TFRs in the context of gravitational waves detection [3].

6 Conclusion

Bilinear TFRs offer a wide panel of tools aimed at analyzing non-stationary signals and simplifying some signal processing operations. The squared magnitude of a linear decompositions is a elementary distribution that has been successfully used in the past.

Unfortunately, despite of their attractive properties, only a few more advanced bilinear distributions have been applied to real-world data. Using a gravitational wave signal as a paradigm, we have sketched how to take advantage of the unitarity and localization properties of these distributions to achieve a more flexible implementation of the matched filtered detection procedure.

References

[1] F. Auger and P. Flandrin, "Improving the readability of time-frequency and time-scale representations by reassignment methods," *IEEE Trans. on Signal Proc.*, **SP-43** (5), pp. 1068–1089, 1995.

[2] E. Chassande-Mottin and P. Flandrin, "On the time-frequency detection of chirps," submitted for publication, 1997.

[3] E. Chassande-Mottin and P. Flandrin, "On the time-frequency detection of chirps and its application to gravitational waves," *Proceedings of GWDAW 2*, Orsay, France, Nov. 1997.

[4] J. Bertrand and P. Bertrand, "A class of affine Wigner distributions with extended covariance properties," *J. Math Phys.*, **33**(7), pp. 2515–2527, 1992.

[5] P. Flandrin, *Temps-Fréquence,* Hermès, Paris, 1993.

[6] L. Cohen, *Time-Frequency Analysis,* NJ: Prentice-Hall, Englewood Cliffs, 1995.

[7] O. Rioul and P. Flandrin, "Time-scale energy distributions: A general class extending wavelet transforms," *IEEE, Trans. on Signal Processing.*, vol. **SP-40**, pp. 1746–1757, July 1992.

[8] P. Flandrin and P. Gonçalvès, "Geometry of affine time-frequency distributions," *App. Comp. Harm. Anal.*, vol. **3**, pp. 10–39, Jan. 1996.

[9] A. Grossmann and J. Morlet, "Decomposition of Hardy functions into square integrable wavelets of constant shape," *SIAM J. Math. Anal.*, vol. **15**(4), pp. 723–736, 1984.

[10] P. Gonçalvès and R. Baraniuk, "Pseudo affine Wigner distributions: definition and kernel formulation," *IEEE, Trans. on Signal Processing.*, to appear, 1997.

[11] K. S. Thorne, "Gravitational radiation," in *300 Years of Gravitation* (S. W. Hawking and W. Israel, *eds.*), pp. 330–458, Cambridge Univ. Press, Cambridge, 1987.

[12] K. Kodera, C. De Villedary, and R. Gendrin, "A new method for the numerical analysis of non-stationary signals," *Phys. Earth and Plan. Int.*, vol. 12, pp. 142–150, 1976.